

1 **Optimization of Non-Coding Regions Improves Protective Efficacy of an**
2 **mRNA SARS-CoV-2 Vaccine in Nonhuman Primates**

3
4 Makda S. Gebre^{1*}, Susanne Rauch^{2*}, Nicole Roth², Jingyou Yu¹, Abishek Chandrashekar¹, Noe B.
5 Mercado¹, Xuan He¹, Jinyan Liu¹, Katherine McMahan¹, Amanda Martinot³, Tori Giffin¹, David
6 Hope¹, Shivani Patel¹, Daniel Sellers¹, Owen Sanborn¹, Julia Barrett¹, Xiaowen Liu⁵, Andrew C.
7 Cole⁵, Laurent Pessaint⁵, Daniel Valentin⁵, Zack Flinchbaugh⁵, Jake Yalley-Ogunro⁵, Jeanne
8 Muench⁵, Renita Brown⁵, Anthony Cook⁵, Elyse Teow⁵, Hanne Andersen⁵, Mark G. Lewis⁵,
9 Stefan O. Mueller², Benjamin Petsch^{*2}, Dan H. Barouch^{*,1,6}

10
11 ¹Center for Virology and Vaccine Research, Beth Israel Deaconess Medical Center, Harvard
12 Medical School, Boston, MA 02215, USA; ²CureVac AG, Tübingen, Germany; ³Tufts
13 University Cummings School of Veterinary Medicine, North Grafton, MA, USA; ⁴Department
14 of Emergency Medicine, Beth Israel Deaconess Medical Center, Boston, MA 02215, USA;
15 ⁵Bioqual, Rockville, MD 20852, USA; ⁶Ragon Institute of MGH, MIT and Harvard, Cambridge,
16 MA, USA

17
18 Corresponding Authors: Dan H. Barouch (dbarouch@bidmc.harvard.edu); Susanne Rauch
19 (Susanne.rauch@curevac.com)

20
21 * These authors contributed equally to the study
22

23 **The CVnCoV (CureVac) mRNA vaccine for SARS-CoV-2 has recently been evaluated in a**
24 **phase 2b/3 efficacy trial in humans. CV2CoV is a second-generation mRNA vaccine with**
25 **optimized non-coding regions and enhanced antigen expression. Here we report a head-to-**
26 **head study of the immunogenicity and protective efficacy of CVnCoV and CV2CoV in**
27 **nonhuman primates. We immunized 18 cynomolgus macaques with two doses of 12 ug of**
28 **lipid nanoparticle formulated CVnCoV, CV2CoV, or sham (N=6/group). CV2CoV induced**
29 **substantially higher binding and neutralizing antibodies, memory B cell responses, and T cell**
30 **responses as compared with CVnCoV. CV2CoV also induced more potent neutralizing**
31 **antibody responses against SARS-CoV-2 variants, including B.1.351 (beta), B.1.617.2 (delta),**
32 **and C.37 (lambda). While CVnCoV provided partial protection against SARS-CoV-2 challenge,**
33 **CV2CoV afforded robust protection with markedly lower viral loads in the upper and lower**
34 **respiratory tract. Antibody responses correlated with protective efficacy. These data**
35 **demonstrate that optimization of non-coding regions can greatly improve the**
36 **immunogenicity and protective efficacy of an mRNA SARS-CoV-2 vaccine in nonhuman**
37 **primates.**

38 The CVnCoV mRNA vaccine (CureVac) has recently reported efficacy results in humans in
39 the Phase 2b/3 HERALD trial in a population that included multiple viral variants. The observed
40 vaccine efficacy against symptomatic COVID-19 was approximately 48% and 53% in the overall
41 study population and in the 18-60 years of age subgroup, respectively [1]. CV2CoV is a second-
42 generation mRNA vaccine that involves modifications of the non-coding regions that were
43 selected based on an empiric screen for improved antigen expression [2, 3]. Both CVnCoV and
44 CV2CoV are based on RNActive® technology [4-7] that consists of non-chemically modified,

45 sequence engineered mRNA, without pseudouridine [6-12]. Both vaccines encode for the same
46 full-length, pre-fusion stabilized SARS-CoV-2 Spike (S) [13, 14] and are encapsulated in lipid
47 nanoparticles (LNP) with identical composition. CV2CoV has been engineered with different non-
48 coding regions flanking the open reading frame, which have previously been shown to improve
49 transgene expression [3] and protection against SARS-CoV-2 in ACE2 transgenic mice [2].
50 Specifically, CV2CoV includes 5' UTR HSD17B4 and 3' UTR PSMB3 elements, followed by a histone
51 stem loop motif and a poly-A sequence (Fig. 1a; see Methods). In this study, we compare head-
52 to-head the immunogenicity and protective efficacy of CVnCoV and CV2CoV against SARS-CoV-2
53 challenge in nonhuman primates.

54

55 **Vaccine Immunogenicity**

56 We immunized 18 cynomolgus macaques intramuscularly with either 12 µg CVnCoV or
57 CV2CoV or sham vaccine (Fig. 1b). Animals were primed at week 0 and boosted at week 4. Sera
58 was isolated from all animals 24h after the first vaccination to assess innate cytokine responses.
59 CV2CoV induced higher levels of IFNα2a, IP-10 and MIP-1 compared with CVnCoV (P = 0.0152, P
60 = 0.0152, P = 0.0411, respectively; Extended Data Fig. 1).

61 Binding antibody responses were assessed by receptor binding domain (RBD)-specific
62 ELISAs at multiple timepoints following immunization [15, 16]. At week 2, binding antibody titers
63 were only detected with CV2CoV and not with CVnCoV (CVnCoV median titer 25 [range 25-25];
64 CV2CoV median titer 799 [range 82-2,010]) (Fig. 2a). One week following the week 4 boost,
65 antibody titers increased in both groups (CVnCoV median titer 48 [range 75-710]); CV2CoV
66 median titer 28,407 [range 2,714-86,541]) (Fig. 2a). By week 8, binding antibody titers increased

67 in the CVnCoV group but were still >50-fold lower than in the CV2CoV group ($P=0.0043$) (CVnCoV
68 median titer 214 [range 47-1,238]; CV2CoV median titer 14,827 [range 2,133-37,079]).

69 Neutralizing antibody (NAb) responses were assessed by pseudovirus neutralization
70 assays initially using the vaccine-matched SARS-CoV-2 wildtype (WT) WA1/2020 strain [15-17].
71 NAb titers followed a similar trend as binding antibody titers (Fig. 2b). At week 2, NAb were only
72 detected with CV2CoV and not with CVnCoV (CVnCoV median titer 20 [range 20-20]; CV2CoV
73 median titer 131 [range 62-578]) (Fig. 2b). One week following the week 4 boost, NAb titers
74 increased (CVnCoV median titer 55 [range 20-302]; CV2CoV median titer 2,758 [range 583-
75 11,941]). By week 8, NAb titers increased in the CVnCoV group but were still >10-fold lower than
76 in the CV2CoV group ($P=0.0043$) (CVnCoV median titer 83 [range 20-335]; CV2CoV median titer
77 991 [range 253-2,765]).

78 At week 6, median NAb titers against the WT WA1/2020, D614G, B.1.1.7 (alpha), and
79 B.1.351 (beta) variants were 456, 121, 101, and 189, respectively, for CVnCoV and were 12,181,
80 4962, 1813, and 755, respectively, for CV2CoV (Fig. 2c). Median NAb titers against C.37 (lambda),
81 B.1.617.1 (kappa), and B.1.617.2 (delta) were 516, 158, and 36, respectively, for CVnCoV and
82 were 1195, 541, and 568, respectively, for CV2CoV (Extended Data Fig. 2). Taken together, these
83 data show that CV2CoV induced substantially higher NAb titers as well against SARS-CoV-2
84 variants compared with CVnCoV.

85 Most SARS-CoV-2 RBD-specific B cells reside within the memory B cell pool [18]. We
86 assessed memory B cell responses in blood from CVnCoV, CV2CoV and sham vaccinated NHPs by
87 flow cytometry [19]. RBD- and Spike-specific memory B cells were detected in the CV2CoV group,
88 but not in the CVnCoV group at week 6 (Fig. 3a, 3b). The cells were not detected at week 1 for

89 both groups (data not shown). T cell responses were assessed by IFN- γ enzyme-linked
90 immunosorbent spot (ELISPOT) assay using pooled S peptides at week 6 in both groups but were
91 higher in the CV2CoV group ($P=0.0065$) (Fig. 3c).

92

93 **Protective Efficacy**

94 All animals were challenged at week 8 with 1.0×10^5 TCID₅₀ SARS-CoV-2 WA1/2020 via the
95 intranasal (IN) and intratracheal (IT) routes. Viral loads were assessed in bronchoalveolar lavage
96 (BAL) and nasal swab (NS) samples collected on days 1, 2, 4, 7 and 10 following challenge by RT-
97 PCR specific for subgenomic mRNA (sgRNA) [20]. High subgenomic RNA levels were observed in
98 BAL and NS in the sham group peak on day 2 and largely resolved by day 10. Sham controls had
99 a peak median of 6.02 (range 4.62–6.81) log₁₀ sgRNA copies/ml in BAL and 7.35 (range 5.84–8.09)
100 log₁₀ sgRNA copies/swab in NS on day 2 (Fig. 4). CVnCoV immunized animals showed a peak
101 median of 4.92 (range 2.40–6.61) log₁₀ sgRNA copies/ml in BAL and 6.42 (range 4.46–7.81) log₁₀
102 sgRNA copies/swab in NS (Fig. 4). CV2CoV immunized animals exhibited a peak median of 2.90
103 (range 1.70–4.64) log₁₀ sgRNA copies/ml in BAL and 3.17 (range 2.59–5.63) log₁₀ sgRNA
104 copies/swab in NS (Fig. 4), with resolution of sgRNA in BAL by day 2 in most animals and by day
105 4 in all animals. Overall, CV2CoV resulted in significantly lower peak viral loads than CVnCoV in
106 both BAL ($P=0.0411$) and NS ($P=0.0087$) (Fig. 5a and b).

107 We next evaluated immune correlates of protection in this study. The log₁₀ ELISA and NAb
108 titers at week 6 inversely correlated with peak log₁₀ sgRNA copies/ml in BAL ($P=0.0008$,
109 $R=-0.7148$ and $P=0.0015$, $R=-0.6912$, respectively, two-sided Spearman rank-correlation test)
110 (Fig. 5, c and e) and with peak sgRNA copies/nasal swab in NS ($P<0.0001$, $R=-0.8346$, and

111 $P < 0.0001$, $R = -0.8766$, respectively, two-sided Spearman rank-correlation test) (Fig. 5, d and f).
112 Consistent with prior observations from our laboratory and others [15, 16, 21], these findings
113 suggest that binding and neutralizing antibody titers are important correlates of protection for
114 these SARS-CoV-2 vaccines in nonhuman primates. Similar correlates of protection were
115 observed with viral loads assessed as area under the curve (AUC) (Extended Data Fig. 3).

116 Following challenge, we observed anamnestic binding and neutralizing antibody
117 responses in the CVnCoV vaccinated animals (Extended Data Fig. 4). We did not observe higher
118 antibody responses in the CV2CoV vaccinated animals following challenge, likely reflecting the
119 robust protection and minimal viral replication in these animals, as we have previously reported
120 [16].

121 On day 10 post-challenge, animals were necropsied, and lung tissues were evaluated by
122 histopathology. Although viral replication had largely resolved by this timepoint, sham animals
123 had higher cumulative lung pathology scores [19] as compared to both CVnCoV and CV2CoV
124 vaccinated animals (CVnCoV $P = 0.0368$; CV2CoV $P = 0.0022$) (Extended Data Fig. 5a). Sham
125 animals also had more lung lobes affected (Extended Data Fig. 5b) and more extensive lung
126 lesions with a greater proportion of lung lobes showing evidence of interstitial inflammation,
127 alveolar inflammatory infiltrates, and type II pneumocyte hyperplasia (Extended Data Fig. 5c-h).
128 No significant differences were observed between the cumulative lung scores between CVnCoV
129 and CV2CoV vaccinated animals on day 10. Pathologic lesions in vaccinated animals were similar
130 to those observed in sham animals (Extended Data Fig. 5i-l) but fewer overall and more focal in
131 distribution.

132

133 **Discussion**

134 CV2CoV elicited substantially higher humoral and cellular immune responses and
135 provided significantly improved protective efficacy against SARS-CoV-2 challenge compared with
136 CVnCoV in macaques. These data suggest that optimization of non-coding elements of the mRNA
137 backbone can substantially improve the immunogenicity and protective efficacy of mRNA
138 vaccines. Both CVnCoV and CV2CoV contain non-modified nucleotides, without pseudouridine
139 or derivatives, and CV2CoV has previously been shown to lead to higher antigen expression than
140 CVnCoV in cell culture [3]. While previous studies in rodents and nonhuman primates have
141 demonstrated protection by CVnCoV [2, 22][23] this was only studied in the lower respiratory
142 tract [22][23]. In the present study, CVnCoV provided only modest reductions in viral loads in
143 BAL and NS compared with sham controls. In contrast, CV2CoV induced >10-fold higher NAb
144 responses than CVnCoV against multiple viral variants and provided >3 log reductions in sgRNA
145 copies/ml in BAL and >4 log reductions in sgRNA copies/swab in NS compared with sham controls.

146 Previous mRNA vaccine clinical trials have demonstrated onset of protective efficacy after
147 the first dose and improved protection after the boost immunization [24, 25]. In the present
148 study, the prime immunization with CV2CoV induced binding and neutralizing antibodies in all
149 macaques by week 2, and these responses increased substantially by 1 week after the boost
150 immunization. Although comparisons with other nonhuman primate studies are difficult due to
151 differences in study designs and laboratory assays, NAb titers induced by CV2CoV appear roughly
152 similar to those reported for previous mRNA vaccines in macaques [26, 27].

153 As previously reported for other vaccines [28-32], NAb titers were lower to certain SARS-
154 CoV-2 variants, including B.1.351 (beta) and B.1.617.2 (delta), than to the parental strain
155 WA1/2020. Although our challenge virus in this study was SARS-CoV-2 WA1/2020, NAb titers
156 elicited by CV2CoV to these viral variants exceeded the threshold that we previously reported as
157 threshold titers for protection (50-100) [17, 19, 21]. However, future studies will be required to
158 assess directly the protective efficacy of CV2CoV against SARS-CoV-2 variants of concern in non-
159 human primates.

160 CV2CoV induced both antigen-specific memory B cell responses and T cell responses.
161 While the correlates of protection in this study were binding and neutralizing antibodies [33, 34],
162 it is likely that CD8⁺ T cells contribute to viral clearance in tissues [35, 36]. We previously reported
163 that depletion of CD8⁺ T cells partially abrogated protective efficacy against SARS-CoV-2 re-
164 challenge in convalescent macaques [21]. Memory B cells may contribute to durability of
165 antibody responses [37, 38], although B cell germinal center responses and durability of
166 protective efficacy following CV2CoV vaccination remain to be determined. Moreover, although
167 this study was not specifically designed as a safety study, it is worth noting that we did not
168 observe any adverse effects following CVnCoV or CV2CoV vaccination, and we did not observe
169 any unexpected or enhanced pathology in the vaccinated animals at necropsy [39].

170 In summary, our data show that optimization of non-coding regions in a SARS-CoV-2
171 mRNA vaccine can substantially improve its immunogenicity against multiple viral variants and
172 enhance protective efficacy against SARS-CoV-2 challenge in nonhuman primates. Improved

173 characteristics of CV2CoV, compared with CVnCoV, could translate into increased efficacy in

174 humans, and clinical trials of CV2CoV are planned.

175

176 **Data availability statement:** All data are available in the manuscript and the supplementary
177 material. This work is licensed under a Creative Commons Attribution 4.0 International (CC BY
178 4.0) license, which permits unrestricted use, distribution, and reproduction in any medium,
179 provided the original work is properly cited. To view a copy of this license, visit
180 <https://creativecommons.org/licenses/by/4.0/>. This license does not apply to
181 figures/photos/artwork or other content included in the article that is credited to a third party;
182 obtain authorization from the rights holder before using such material.

183 **Acknowledgements:** We thank Sarah Gardner, Gabriella Kennedy, and Rachael Edmonston for
184 their generous assistance. We thank Domenico Maione and Marie-Thérèse Martin for critically
185 reading the manuscript.

186 **Funding Source:** This work was supported by CureVac AG and the German Federal Ministry of
187 Education and Research (BMBF; grant 01KI20703). Development of CV2CoV is carried out in a
188 collaboration of CureVac AG and GSK.

189 **Author contributions:** S.R., B.P., S.O.M., N.R. and D.H.B. designed the study. M.S.G., J.Y., A.C., N.
190 M., X. H., J. L., K. M., A. M., T.G., D.H., S.P., D.S., O.S., and J.B. performed immunologic and
191 virologic assays. X.L. and A.C.C. performed cytokine analysis. L.P., D.V., Z.F., J.Y., J.M., R.B., A.C.,
192 E.T., H.A. and M.L. led the clinical care of the animals. M.S.G. and D.H.B. wrote the paper with all
193 coauthors.

194 **Competing interests:** S.R., B.P., N.R., and S.O.M. are employees of CureVac AG, Tübingen,
195 Germany, a publicly listed company developing mRNA-based vaccines and immunotherapeutics.
196 Authors may hold shares in the company. S.R. and B.P. and N.R. are inventors on several patents
197 on mRNA vaccination and use thereof. The other authors declare no competing interests.

198 **Corresponding authors:** Dan H. Barouch, M.D.; Email: dbarouch@bidmc.harvard.edu; Susanne

199 Rauch, Ph.D., Email: Susanne.rauch@curevac.com

200

201 **References**

- 202 1. AG, C., *CureVac Final Data from Phase 2b/3 Trial of First-Generation COVID-19 Vaccine*
203 *Candidate, CVnCoV, Demonstrates Protection in Age Group of 18 to 60*
204 [https://www.curevac.com/en/2021/06/30/curevac-final-data-from-phase-2b-3-trial-of-](https://www.curevac.com/en/2021/06/30/curevac-final-data-from-phase-2b-3-trial-of-first-generation-covid-19-vaccine-candidate-cvncov-demonstrates-protection-in-age-group-of-18-to-60/)
205 [first-generation-covid-19-vaccine-candidate-cvncov-demonstrates-protection-in-age-](https://www.curevac.com/en/2021/06/30/curevac-final-data-from-phase-2b-3-trial-of-first-generation-covid-19-vaccine-candidate-cvncov-demonstrates-protection-in-age-group-of-18-to-60/)
206 [group-of-18-to-60/](https://www.curevac.com/en/2021/06/30/curevac-final-data-from-phase-2b-3-trial-of-first-generation-covid-19-vaccine-candidate-cvncov-demonstrates-protection-in-age-group-of-18-to-60/).
- 207 2. Hoffmann, D., et al., *CVnCoV and CV2CoV protect human ACE2 transgenic mice from*
208 *ancestral B BavPat1 and emerging B.1.351 SARS-CoV-2*. *Nat Commun*, 2021. **12**(1): p.
209 4048.
- 210 3. Nicole Roth, J.S., Donata Hoffmann, Moritz Thran, Andreas Thess, Stefan O. Mueller,
211 Benjamin Petsch and Susanne Rauch, *CV2CoV, an enhanced mRNA-based SARS-CoV-2*
212 *vaccine candidate, supports higher protein expression and improved immunogenicity in*
213 *rats*. *bioRxiv*, 2021.
- 214 4. Hoerr, I., et al., *In vivo application of RNA leads to induction of specific cytotoxic T*
215 *lymphocytes and antibodies*. *Eur J Immunol*, 2000. **30**(1): p. 1-7.
- 216 5. Fotin-Mleczek, M., et al., *Highly potent mRNA based cancer vaccines represent an*
217 *attractive platform for combination therapies supporting an improved therapeutic*
218 *effect*. *J Gene Med*, 2012. **14**(6): p. 428-39.
- 219 6. Fotin-Mleczek, M., et al., *Messenger RNA-based vaccines with dual activity induce*
220 *balanced TLR-7 dependent adaptive immune responses and provide antitumor activity*. *J*
221 *Immunother*, 2011. **34**(1): p. 1-15.
- 222 7. Kubler, H., et al., *Self-adjuvanted mRNA vaccination in advanced prostate cancer*
223 *patients: a first-in-man phase I/IIa study*. *J Immunother Cancer*, 2015. **3**: p. 26.
- 224 8. Lutz, J., et al., *Unmodified mRNA in LNPs constitutes a competitive technology for*
225 *prophylactic vaccines*. *NPJ Vaccines*, 2017. **2**: p. 29.
- 226 9. Stitz, L., et al., *A thermostable messenger RNA based vaccine against rabies*. *PLoS Negl*
227 *Trop Dis*, 2017. **11**(12): p. e0006108.
- 228 10. Schnee, M., et al., *An mRNA Vaccine Encoding Rabies Virus Glycoprotein Induces*
229 *Protection against Lethal Infection in Mice and Correlates of Protection in Adult and*
230 *Newborn Pigs*. *PLoS Negl Trop Dis*, 2016. **10**(6): p. e0004746.
- 231 11. Petsch, B., et al., *Protective efficacy of in vitro synthesized, specific mRNA vaccines*
232 *against influenza A virus infection*. *Nat Biotechnol*, 2012. **30**(12): p. 1210-6.
- 233 12. Aldrich, C., et al., *Proof-of-concept of a low-dose unmodified mRNA-based rabies vaccine*
234 *formulated with lipid nanoparticles in human volunteers: A phase 1 trial*. *Vaccine*, 2021.
235 **39**(8): p. 1310-1318.
- 236 13. Pallesen, J., et al., *Immunogenicity and structures of a rationally designed prefusion*
237 *MERS-CoV spike antigen*. *Proc Natl Acad Sci U S A*, 2017. **114**(35): p. E7348-E7357.
- 238 14. Kirchdoerfer, R.N., et al., *Stabilized coronavirus spikes are resistant to conformational*
239 *changes induced by receptor recognition or proteolysis*. *Sci Rep*, 2018. **8**(1): p. 15701.
- 240 15. Yu, J., et al., *DNA vaccine protection against SARS-CoV-2 in rhesus macaques*. *Science*,
241 2020. **369**(6505): p. 806-811.
- 242 16. Mercado, N.B., et al., *Single-shot Ad26 vaccine protects against SARS-CoV-2 in rhesus*
243 *macaques*. *Nature*, 2020. **586**(7830): p. 583-588.

- 244 17. Chandrashekar, A., et al., *SARS-CoV-2 infection protects against rechallenge in rhesus*
245 *macaques*. *Science*, 2020. **369**(6505): p. 812-817.
- 246 18. He, X., et al., *Low-Dose Ad26.COV2.S Protection Against SARS-CoV-2 Challenge in Rhesus*
247 *Macaques*. *Cell*, 2021.
- 248 19. He, X., et al., *Low-dose Ad26.COV2.S protection against SARS-CoV-2 challenge in rhesus*
249 *macaques*. *Cell*, 2021. **184**(13): p. 3467-3473 e11.
- 250 20. Dagotto, G., et al., *Comparison of Subgenomic and Total RNA in SARS-CoV-2 Challenged*
251 *Rhesus Macaques*. *J Virol*, 2021.
- 252 21. McMahan, K., et al., *Correlates of protection against SARS-CoV-2 in rhesus macaques*.
253 *Nature*, 2021. **590**(7847): p. 630-634.
- 254 22. Rauch, S., et al., *mRNA-based SARS-CoV-2 vaccine candidate CVnCoV induces high levels*
255 *of virus-neutralising antibodies and mediates protection in rodents*. *NPJ Vaccines*, 2021.
256 **6**(1): p. 57.
- 257 23. Susanne Rauch, K.G., Yper Hall, Francisco J. Salguero, Mike J. Dennis, Fergus V. Gleeson,
258 Debbie Harris, Catherine Ho, Holly E. Humphries, Stephanie Longet, Didier Ngabo,
259 Jemma Paterson, Emma L. Rayner, Kathryn A. Ryan, Sally Sharpe, Robert J. Watson,
260 Stefan O. Mueller, Benjamin Petsch, Miles W. Carroll *mRNA vaccine CVnCoV protects*
261 *non-human primates from SARS-CoV-2 challenge infection*. *bioRxiv*, 2020.
- 262 24. Polack, F.P., et al., *Safety and Efficacy of the BNT162b2 mRNA Covid-19 Vaccine*. *N Engl J*
263 *Med*, 2020. **383**(27): p. 2603-2615.
- 264 25. Baden, L.R., et al., *Efficacy and Safety of the mRNA-1273 SARS-CoV-2 Vaccine*. *N Engl J*
265 *Med*, 2021. **384**(5): p. 403-416.
- 266 26. Corbett, K.S., et al., *Evaluation of the mRNA-1273 Vaccine against SARS-CoV-2 in*
267 *Nonhuman Primates*. *N Engl J Med*, 2020. **383**(16): p. 1544-1555.
- 268 27. Vogel, A.B., et al., *BNT162b vaccines protect rhesus macaques from SARS-CoV-2*. *Nature*,
269 2021. **592**(7853): p. 283-289.
- 270 28. Liu, C., et al., *Reduced neutralization of SARS-CoV-2 B.1.617 by vaccine and convalescent*
271 *serum*. *Cell*, 2021.
- 272 29. Haas, E.J., et al., *Impact and effectiveness of mRNA BNT162b2 vaccine against SARS-*
273 *CoV-2 infections and COVID-19 cases, hospitalisations, and deaths following a*
274 *nationwide vaccination campaign in Israel: an observational study using national*
275 *surveillance data*. *Lancet*, 2021. **397**(10287): p. 1819-1829.
- 276 30. Wu, K., et al., *Serum Neutralizing Activity Elicited by mRNA-1273 Vaccine*. *N Engl J Med*,
277 2021. **384**(15): p. 1468-1470.
- 278 31. Wibmer, C.K., et al., *SARS-CoV-2 501Y.V2 escapes neutralization by South African COVID-*
279 *19 donor plasma*. *Nat Med*, 2021. **27**(4): p. 622-625.
- 280 32. Wall, E.C., et al., *Neutralising antibody activity against SARS-CoV-2 VOCs B.1.617.2 and*
281 *B.1.351 by BNT162b2 vaccination*. *Lancet*, 2021. **397**(10292): p. 2331-2333.
- 282 33. Philipp, M. and G. Santibanez, *Preference of respiratory phases to perform reaction time*
283 *tasks*. *Act Nerv Super (Praha)*, 1988. **30**(2): p. 153-5.
- 284 34. Feng, S., et al., *Correlates of protection against symptomatic and asymptomatic SARS-*
285 *CoV-2 infection*. *medRxiv*, 2021: p. 2021.06.21.21258528.

- 286 35. Lafon, E., et al., *Potent SARS-CoV-2-Specific T Cell Immunity and Low Anaphylatoxin*
287 *Levels Correlate With Mild Disease Progression in COVID-19 Patients*. *Front Immunol*,
288 2021. **12**: p. 684014.
- 289 36. Schmidt, M.E. and S.M. Varga, *The CD8 T Cell Response to Respiratory Virus Infections*.
290 *Front Immunol*, 2018. **9**: p. 678.
- 291 37. Abayasingam, A., et al., *Long-term persistence of RBD(+) memory B cells encoding*
292 *neutralizing antibodies in SARS-CoV-2 infection*. *Cell Rep Med*, 2021. **2**(4): p. 100228.
- 293 38. Dan, J.M., et al., *Immunological memory to SARS-CoV-2 assessed for up to 8 months*
294 *after infection*. *Science*, 2021. **371**(6529).
- 295 39. Graham, B.S., *Rapid COVID-19 vaccine development*. *Science*, 2020. **368**(6494): p. 945-
296 946.
- 297 40. Yu, J., et al., *Deletion of the SARS-CoV-2 Spike Cytoplasmic Tail Increases Infectivity in*
298 *Pseudovirus Neutralization Assays*. *J Virol*, 2021.
- 299 41. Wolfel, R., et al., *Virological assessment of hospitalized patients with COVID-2019*.
300 *Nature*, 2020. **581**(7809): p. 465-469.
- 301

302

303 **Materials and Methods**

304 **mRNA vaccines**

305 The two mRNA vaccines, CVnCoV and CV2CoV, are based on CureVac's RnActive®
306 platform (claimed and described in e.g. WO2002098443 and WO2012019780) and do not include
307 chemically modified nucleosides. They are comprised of a 5' cap1 structure, a GC-enriched open
308 reading frame (ORF), 3' UTR and a vector-encoded poly-A stretch. CVnCoV contains a cleanCap
309 (Trilink), parts of the 3' UTR of the Homo sapiens alpha haemoglobin gene as 3' UTR, followed by
310 a poly-A (64) stretch, a polyC (30) stretch and a histone stem loop [22, 23]. CV2CoV has previously
311 been described to contain a cleanCap followed by 5' UTR from the human hydroxysteroid 17-
312 beta dehydrogenase 4 gene (HSD17B4) and a 3' UTR from human proteasome 20S subunit beta
313 3 gene (PSMB3), followed by a histone stem loop and a poly-A (100) stretch [3]. Both constructs
314 were encapsulated in lipid nanoparticles (LNP) by Acuitas Therapeutics (Vancouver, Canada)
315 (CV2CoV) or Polymun Scientific Immunbiologische Forschung GmbH (Klosterneuburg, Austria)
316 (CVnCoV). LNPs are composed of ionizable amino lipid, phospholipid, cholesterol, and a
317 PEGylated lipid; compositions for CVnCoV and CV2CoV are identical. Both mRNAs encode for
318 SARS-CoV-2 full length spike protein containing stabilizing K986P and V987P mutations (NCBI
319 Reference Sequence NC_045512.2).

320

321 **Animals and study design**

322 18 cynomolgus macaques were randomly assigned to three groups. Animals received
323 either CVnCoV (N=6) or CV2CoV (N=6) mRNA vaccines or were designated as sham controls (N=6).
324 The mRNA vaccines were administered at a 12 µg dose, intramuscularly, in the left quadriceps on

325 day 0. Boost immunizations were similarly administered at week 4. At week 8, all animals were
326 challenged with 1.0×10^5 TCID₅₀ SARS-CoV-2 derived from USA-WA1/2020 (NR-52281; BEI
327 Resources) [17]. Challenge virus was administered as 1 ml by the intranasal (IN) route (0.5 ml in
328 each nare) and 1 ml by the intratracheal (IT) route. All animals were sacrificed 10 days post
329 challenge. Immunologic and virologic assays were performed blinded. All animals were housed
330 at Bioqual, Inc. (Rockville, MD). All animal studies were conducted in compliance with all relevant
331 local, state, and federal regulations and were approved by the Bioqual Institutional Animal Care
332 and Use Committee (IACUC).

333

334 **Cytokine analyses**

335 Serum levels of 19 analytes that have been associated with immune response to viral
336 infection were tested using U-PLEX Viral Combo 1 (NHP) kit (K15069L-1) from Meso Scale
337 Discovery (MSD, Rockville, MD). The 19 analytes and their detection limits (LLODs) are G-CSF (1.5
338 pg/mL), GM-CSF (0.12 pg/mL), IFN- α 2a (1.7 pg/mL), IFN- γ (1.7 pg/mL), IL-1RA (1.7 pg/mL), IL-1 β
339 (0.15 pg/mL), IL-4 (0.06 pg/mL), IL-5 (0.24 pg/mL), IL-6 (0.33 pg/mL), IL-7 (1.5 pg/mL) and IL-8
340 (0.15 pg/mL), IL-9 (0.14 pg/mL), IL-10 (0.14 pg/mL), IL-12p70 (0.54 pg/mL), IP-10 (0.49 pg/mL),
341 MCP-1 (0.74 pg/mL), MIP-1 α (7.7 pg/mL), TNF- α (0.54 pg/mL) and VEGF-A (2.0pg/mL). All serum
342 samples were assayed in duplicate. Assay was done by the Metabolism and Mitochondrial
343 Research Core (Beth Israel Deaconess Medical Center, Boston, MA) following manufacture's
344 instruction. The assay plates were read by MESO QUICKPLEX SQ 120 instrument and data were
345 analyzed by DISCOVERY WORKBENCH® 4.0 software.

346

347 **Enzyme-linked immunosorbent assay (ELISA)**

348 RBD-specific binding antibodies were assessed by ELISA as described [16, 17]. Briefly, 96-
349 well plates were coated with 1 μ g/ml SARS-CoV-2 RBD protein (40592-VNAH, SinoBiological) in 1X
350 DPBS and incubated at 4°C overnight. After incubation, plates were washed once with wash
351 buffer (0.05% Tween 20 in 1 X DPBS) and blocked with 350 μ L Casein block/well for 2–3 h at room
352 temperature. After incubation, block solution was discarded, and plates were blotted dry. Serial
353 dilutions of heat-inactivated serum diluted in casein block were added to wells and plates were
354 incubated for 1 h at room temperature. Next, the plates were washed three times and incubated
355 for 1 h with a 1:1000 dilution of anti-macaque IgG HRP (NIH NHP Reagent Program) at room
356 temperature in the dark. Plates were then washed three more times, and 100 μ L of SeraCare KPL
357 TMB SureBlue Start solution was added to each well; plate development was halted by the
358 addition of 100 μ L SeraCare KPL TMB Stop solution per well. The absorbance at 450nm was
359 recorded using a VersaMax or Omega microplate reader. ELISA endpoint titers were defined as
360 the highest reciprocal serum dilution that yielded an absorbance > 0.2. Log₁₀ endpoint titers are
361 reported. Immunologic assays were performed blinded.

362

363 **Pseudovirus neutralization assay**

364 The SARS-CoV-2 pseudoviruses expressing a luciferase reporter gene were generated as
365 described previously [15, 40]. Briefly, the packaging plasmid psPAX2 (AIDS Resource and Reagent
366 Program), luciferase reporter plasmid pLenti-CMV Puro-Luc (Addgene), and Spike protein
367 expressing pcDNA3.1-SARS CoV-2 Δ CT of variants were co-transfected into HEK293T cells by
368 lipofectamine 2000 (ThermoFisher). Pseudoviruses of SARS-CoV-2 variants were generated by

369 using WA1/2020 strain (Wuhan/WIV04/2019, GISAID accession ID: EPI_ISL_402124), D614G
370 mutation, B.1.1.7 variant (GISAID accession ID: EPI_ISL_601443), B.1.351 variant (GISAID
371 accession ID: EPI_ISL_712096), C37 variant (GenBank ID: QRX62290), B.1.671.1 variant (GISAID
372 accession ID: EPI_ISL_1384866) and B.1.617.2 variant (GISAID accession ID: EPI_ISL_2020950).
373 The supernatants containing the pseudotype viruses were collected 48 h post-transfection, which
374 were purified by centrifugation and filtration with 0.45 µm filter. To determine the neutralization
375 activity of the plasma or serum samples from participants, HEK293T-hACE2 cells were seeded in
376 96-well tissue culture plates at a density of 1.75×10^4 cells/well overnight. Three-fold serial
377 dilutions of heat inactivated serum or plasma samples were prepared and mixed with 50 µL of
378 pseudovirus. The mixture was incubated at 37°C for 1 h before adding to HEK293T-hACE2 cells.
379 48 h after infection, cells were lysed in Steady-Glo Luciferase Assay (Promega) according to the
380 manufacturer's instructions. SARS-CoV-2 neutralization titers were defined as the sample dilution
381 at which a 50% reduction in relative light unit (RLU) was observed relative to the average of the
382 virus control wells.

383

384 **B cell immunophenotyping**

385 Fresh PBMCs were stained with Aqua live/dead dye (Invitrogen) for 20 min, washed with
386 2% FBS/DPBS buffer, and suspended in 2% FBS/DPBS buffer with Fc Block (BD) for 10 min,
387 followed by staining with monoclonal antibodies against CD45 (clone D058-1283, BUV805), CD3
388 (clone SP34.2 , APC-Cy7), CD7 (clone M-T701, Alexa700), CD123 (clone 6H6, Alexa700), CD11c
389 (clone 3.9, Alexa700), CD20 (clone 2H7, PE-Cy5), IgA (goat polyclonal antibodies, APC), IgG (clone
390 G18-145, BUV737), IgM (clone G20-127, BUV396), IgD (goat polyclonal antibodies, PE), CD80

391 (clone L307.4, BV786), CD95 (clone DX2, BV711), CD27 (clone M-T271, BUV563), CD21 (clone B-
392 ly4, BV605), CD14 (clone M5E2, BV570) and CD138 (clone DL-101, PE-CF594). Cells were also
393 stained with SARS-CoV-2 antigens including biotinylated SARS-CoV-2 RBD protein (Sino
394 Biological) and full-length SARS-CoV-2 Spike protein (Sino Biological) labeled with FITC and
395 DyLight 405 (DyLight® 405 Conjugation Kit, FITC Conjugation Kit, Abcam), at 4 °C for 30 min. After
396 staining, cells were washed twice with 2% FBS/DPBS buffer, followed by incubation with BV650
397 streptavidin (BD Pharmingen) for 10min, then washed twice with 2% FBS/DPBS buffer. After
398 staining, cells were washed and fixed by 2% paraformaldehyde. All data were acquired on a BD
399 FACSymphony flow cytometer. Subsequent analyses were performed using FlowJo software
400 (Treestar, v.9.9.6). Immunologic assays were performed blinded.

401

402 **IFN- γ enzyme-linked immunospot (ELISPOT) assay**

403 ELISPOT plates were coated with mouse anti-human IFN- γ monoclonal antibody from BD
404 Pharmingen at a concentration of 5 μ g/well overnight at 4°C. Plates were washed with DPBS
405 containing 0.25% Tween 20, and blocked with R10 media (RPMI with 11% FBS and 1.1% penicillin-
406 streptomycin) for 1 h at 37°C. The Spike 1 and Spike 2 peptide pools (JPT Peptide Technologies,
407 custom made) used in the assay contain 15 amino acid peptides overlapping by 11 amino acids
408 that span the protein sequence and reflect the N- and C- terminal halves of the protein,
409 respectively. Spike 1 and Spike 2 peptide pools were prepared at a concentration of 2 μ g/well,
410 and 200,000 cells/well were added. The peptides and cells were incubated for 18–24 h at 37°C.
411 All steps following this incubation were performed at room temperature. The plates were washed
412 with ELISPOT wash buffer and incubated for 2 h with Rabbit polyclonal anti-human IFN- γ Biotin

413 from U-Cytech (1 µg/mL). The plates are washed a second time and incubated for 2 h with
414 Streptavidin-alkaline phosphatase antibody from Southern Biotechnology (1 µg/mL). The final
415 wash was followed by the addition of Nitro-blue Tetrazolium Chloride/5-bromo-4-chloro 3
416 'indolyl phosphate p-toluidine salt (NBT/BCIP chromagen) substrate solution (Thermo Scientific)
417 for 7 min. The chromagen was discarded and the plates were washed with water and dried in a
418 dim place for 24 h. Plates were scanned and counted on a Cellular Technologies Limited
419 Immunospot Analyzer.

420

421 **Subgenomic RT-PCR assay**

422 SARS-CoV-2 E gene subgenomic RNA (sgRNA) was assessed by RT-PCR using primers and
423 probes as previously described [15, 17]. A standard was generated by first synthesizing a gene
424 fragment of the subgenomic E gene [41]. The gene fragment was subsequently cloned into a
425 pcDNA3.1+ expression plasmid using restriction site cloning (Integrated DNA Technologies). The
426 insert was *in vitro* transcribed to RNA using the AmpliCap-Max T7 High Yield Message Maker Kit
427 (CellScript). Log dilutions of the standard were prepared for RT-PCR assays ranging from 1×10^{10}
428 copies to 1×10^{-1} copies. Viral loads were quantified from bronchoalveolar lavage (BAL) fluid and
429 nasal swabs (NS). RNA extraction was performed on a QIAcube HT using the IndiSpin QIAcube HT
430 Pathogen Kit according to manufacturer's specifications (Qiagen). The standard dilutions and
431 extracted RNA samples were reverse transcribed using SuperScript VILO Master Mix (Invitrogen)
432 following the cycling conditions described by the manufacturer. A Taqman custom gene
433 expression assay (Thermo Fisher Scientific) was designed using the sequences targeting the E
434 gene sgRNA [41]. The sequences for the custom assay were as follows, forward primer,

435 sgLeadCoV2.Fwd: CGATCTCTGTAGATCTGTTCTC, E_Sarbeco_R: ATATTGCAGCAGTACGCACACA,
436 E_Sarbeco_P1 (probe): VIC-ACACTAGCCATCCTTACTGCGCTTCG-MGBNFQ. Reactions were carried
437 out in duplicate for samples and standards on the QuantStudio 6 and 7 Flex Real-Time PCR
438 Systems (Applied Biosystems) with the thermal cycling conditions: initial denaturation at 95°C for
439 20 seconds, then 45 cycles of 95°C for 1 second and 60°C for 20 seconds. Standard curves were
440 used to calculate subgenomic RNA copies per ml or per swab. The quantitative assay sensitivity
441 was determined as 50 copies per ml or per swab.

442

443 **Histopathology**

444 At time of fixation, lungs were suffused with 10% formalin to expand the alveoli. All
445 tissues were fixed in 10% formalin and blocks sectioned at 5 µm. Slides were baked for 30-60 min
446 at 65 degrees, deparaffinized in xylene, rehydrated through a series of graded ethanol to distilled
447 water, then stained with hematoxylin and eosin (H&E). Blinded histopathological evaluation was
448 performed by a board-certified veterinary pathologist (AJM).

449

450 **Statistical analyses**

451 Statistical analyses were performed using GraphPad Prism (version 9.0) software
452 (GraphPad Software) and comparison between groups was performed using a two-tailed
453 nonparametric Mann-Whitney U t test. P-values of less than 0.05 were considered significant.
454 Correlations were assessed by two-sided Spearman rank-correlation tests.

455

456 **Figure Legends**

457

458 **Figure 1. (a) mRNA vaccine design and (b) NHP vaccine study schema**

459

460 **Figure 2. CV2CoV elicits high levels of binding and neutralizing antibody responses in NHPs.**

461 NHPs (6/group) were vaccinated twice with 12 μ g of CVnCoV or CV2CoV on d0 and d28 or
462 remained untreated as negative controls (sham). (a) Titers of RBD binding antibodies and (b)
463 pseudovirus neutralizing antibodies against ancestral SARS-CoV-2 strain were evaluated at
464 different time points post first (week 0, 1, 2 and 4) and second (week 5, 6 and 8) vaccinations. (c)
465 Sera isolated on d42 (week 6) were analyzed for pseudovirus neutralizing antibodies titers against
466 the ancestral WA/2020 (WT) strain, virus featuring the D614G mutation, and variants including
467 B.1.1.7 (Alpha) and B.1.351 (Beta). Each dot represents an individual animal, bars depict the
468 median and the dotted line shows limit of detection.

469

470 **Figure 3. CV2CoV induces memory B cell and T cell immune responses in on day 42.** PBMCs from

471 negative control (sham), CVnCoV or CV2CoV vaccinated animals isolated on d42 of the
472 experiment were stained for (a) RBD and (b) Spike-specific activated memory B cells and analyzed
473 by high-parameter flow cytometry. IFN γ responses to pooled spike peptides were analyzed via
474 ELISPOT (c). Each dot represents an individual animal, bars depict the median and the dotted line
475 shows limit of detection. PBMC = peripheral blood mononuclear cell; SFC = spot forming cells

476

477

478 **Figure 4. CV2CoV protects NHPs from challenge infection.** Negative control (sham) or animals
479 vaccinated on d0 and d28 of the experiment with 12µg of CVnCoV or CV2CoV as indicated were
480 subjected to challenge infection using 1.0×10^5 TCID₅₀ SARS-CoV-2 via intranasal (IN) and
481 intratracheal (IT) routes. BAL (**a**) and nasal swab samples (**b**) collected on days 1, 2, 4, 7 and 10
482 post-challenge were analyzed for levels of replicating virus by RT-PCR specific for subgenomic
483 mRNA (sgRNA). Thin black lines represent an individual animal, thick red lines depict the median
484 and the dotted line shows limit of detection. BAL = bronchoalveolar lavage

485

486 **Figure 5. Titers of binding and neutralizing antibody titers elicited upon CVnCoV and CV2CoV**
487 **vaccination correlate with protection against SARS-CoV-2.** Summary of peak viral loads
488 following SARS-CoV-2 challenge in BAL and Nasal Swab (left panels **a** and **b**); antibody correlates
489 of protection for binding antibodies (middle panels in **c** and **d**) and neutralizing antibodies (right
490 panels **e** and **f**). NAbs = neutralizing antibodies, BAL = bronchoalveolar lavage NS = nasal swab

491

492

493

494 **Extended Data Figure Legends**

495

496 **Extended Data Figure. 1. mRNA vaccination leads to innate cytokine induction in the serum of**

497 **NHPs 24h post immunization.** Sera isolated 24h post first injection were analyzed for a panel of

498 19 cytokines associated with viral infection using a U-PLEX Viral Combo kit from Meso Scale

499 Discovery. Changes in cytokine levels above the detection limits were detectable for 9 cytokines.

500 Each dot represents an individual animal, bars depict the median and the dotted line shows limit

501 of detection. Statistical analysis was performed using Mann-Whitney test.

502

503 **Extended Data Figure. 2. CV2CoV elicits high levels of binding and neutralizing antibody**

504 **responses in NHPs.** NHPs (6/group) were vaccinated twice with 12 μ g of CVnCoV or CV2CoV on

505 d0 and d28 or remained untreated as negative controls (sham). Sera isolated on d42 (week 6)

506 were analyzed for pseudovirus neutralizing antibodies titers against the ancestral WA/2020 (WT)

507 strain, C.37 (Lambda), B.1.617.1 (Kappa) and B.1.617.2 (Delta). Each dot represents an individual

508 animal, bars depict the median and the dotted line shows limit of detection.

509

510 **Extended Data Figure. 3. Titers of binding and neutralizing antibody titers elicited upon CVnCoV**

511 **and CV2CoV vaccination correlate with protection against SARS-CoV-2.** Summary of area under

512 curve (AUC) viral load values following SARS-CoV-2 challenge in BAL and Nasal Swab (left panels

513 **a** and **b**); antibody correlates of protection for binding antibodies (middle panels in **c** and **d**) and

514 neutralizing antibodies (right panels **e** and **f**). NABs = neutralizing antibodies, BAL =

515 bronchoalveolar lavage NS = nasal swab

516

517 **Extended Data Figure. 4. Post-challenge binding and neutralizing antibody responses of NHPs.**

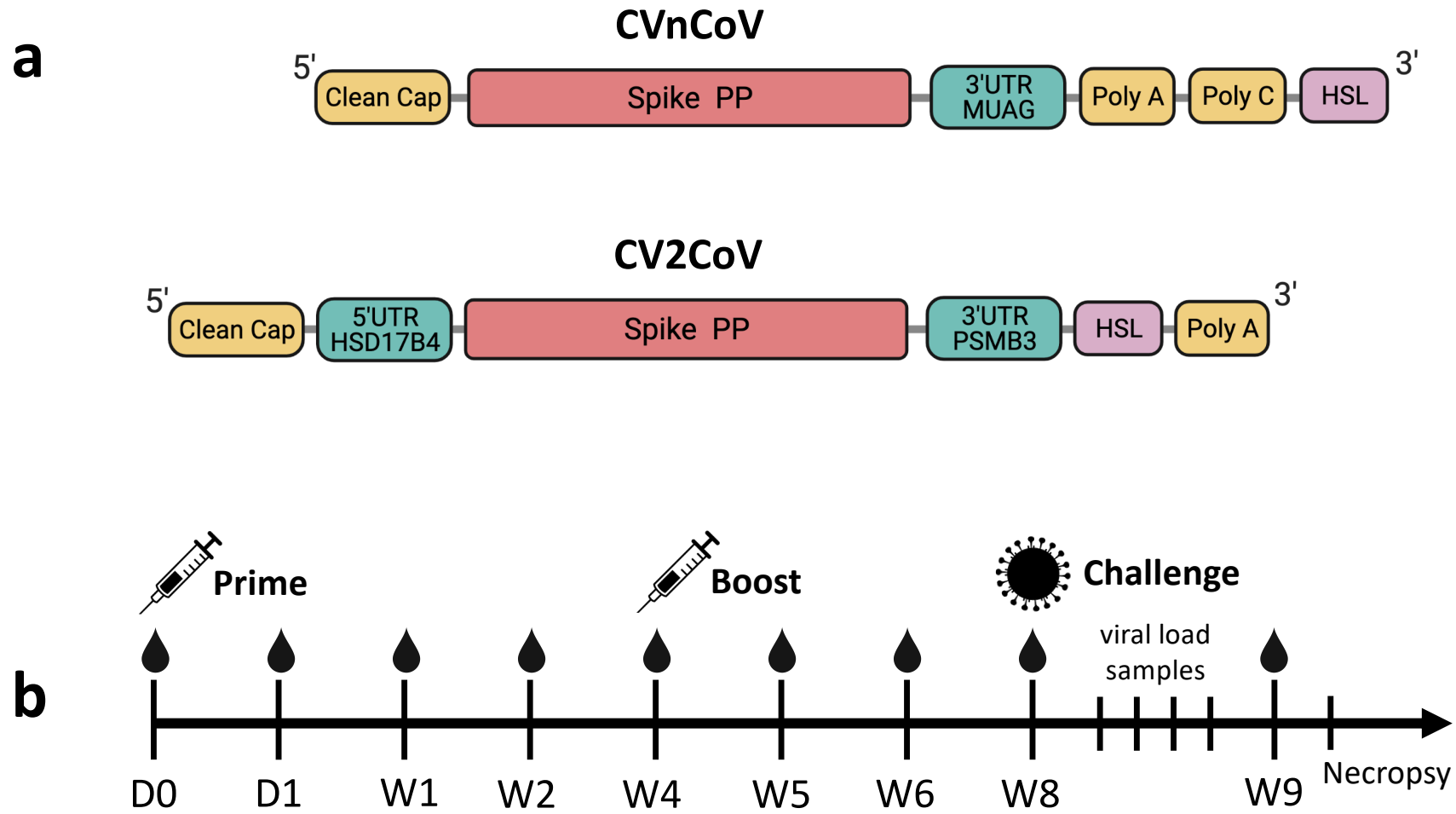
518 Negative control (sham) or animals vaccinated on d0 and d28 of the experiment with 12µg of
519 CVnCoV or CV2CoV as indicated were subjected to challenge infection using 1.0×10^5 TCID₅₀ SARS-
520 CoV-2 via intranasal (IN) and intratracheal (IT) routes.). **(a)** Titers of RBD binding antibodies and
521 **(b)** pseudovirus neutralizing antibodies against ancestral SARS-CoV-2 strain were evaluated
522 before (week 8) and a week after challenge infection (week 9). Each dot represents an individual
523 animal, bars depict the median and the dotted line shows limit of detection. NAbs= neutralizing
524 antibodies

525

526 **Extended Data Figure. 5: CVnCoV and CV2CoV protect the lungs from pathological changes**

527 **upon viral challenge.** Eight lung lobes (4 sections from right and left, caudal to cranial) were
528 assessed and scored (1-4) for each of the following lesions: 1) Interstitial inflammation and septal
529 thickening 2) Eosinophilic interstitial infiltrate 3) Neutrophilic interstitial infiltrate 4) Hyaline
530 membranes 5) Interstitial fibrosis 6) Alveolar infiltrate, macrophage 7) Alveolar/Bronchoalveolar
531 infiltrate, neutrophils 8) Syncytial cells 9) Type II pneumocyte hyperplasia 10) Broncholar
532 infiltrate, macrophage 11) Broncholar infiltrate, neutrophils 12) BALT hyperplasia 13)
533 Bronchiolar/peribronchiolar inflammation 14) Perivascular, mononuclear infiltrates 15) Vessels,
534 endothelialitis. Each feature assessed was assigned a score of 0= no significant findings;
535 1=minimal; 2= mild; 3=moderate; 4=marked/severe. **(a)** Cumulative scores per animal **(b)**
536 Cumulative scores per lung lobe. Individual animals are represented by symbols. Representative
537 histopathology from sham vaccinated (**c-h**), CnVCoV vaccinated (**i, j**), and Cv2CoV vaccinated (**k**,

538 **l)** animals showing (**c, d**, inset) alveolar macrophage infiltrate, (**e, f**, inset) syncytial cells
539 (arrowheads) and type II pneumocyte hyperplasia, inset (**g, h**, inset) bronchiolar epithelial
540 necrosis with neutrophilic infiltrates (**i**) alveolar neutrophilic infiltrate and alveolar septal
541 thickening (**j**) focal consolidation with inflammation composed of macrophages, neutrophils, and
542 syncytial cells (**k**) focal pneumocyte hyperplasia, syncytial cells and inflammatory infiltrates (**l**)
543 peribronchiolar inflammation. Scale bars: 100 microns (**c**), 50 microns (**e, g**) 20 microns (**i-l**). BAL
544 bronchus associated lymphoid tissue.



Groups (N=6)	Vaccines	Antigen	Dose	Route
I	Sham	Sham	Sham	Sham
II	CVnCoV	Full length Spike (K986P, V987P)	12 μ g	I.M.
III	CV2CoV	Full length Spike (K986P, V987P)	12 μ g	I.M.

Figure 1

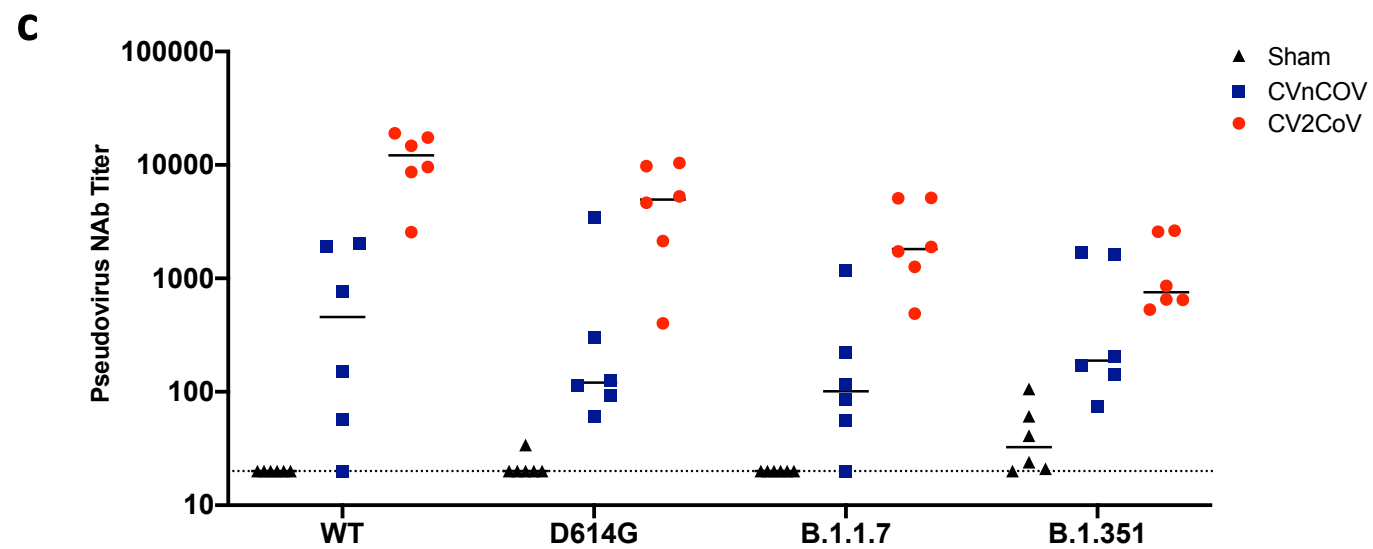
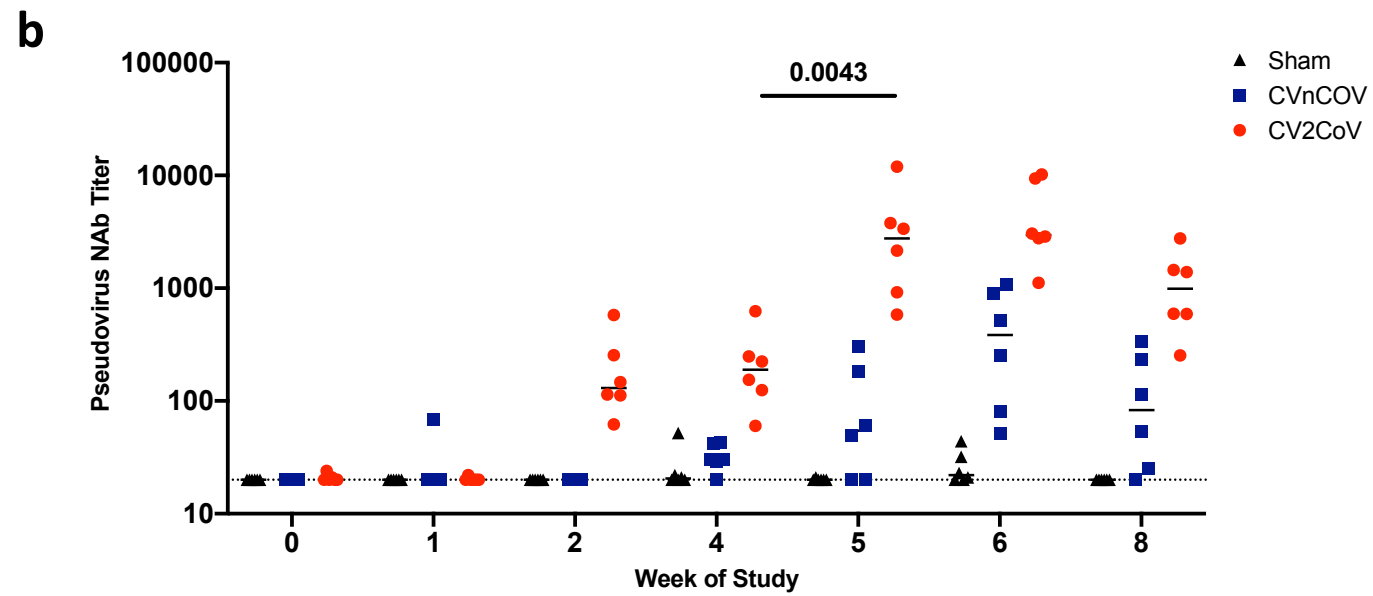
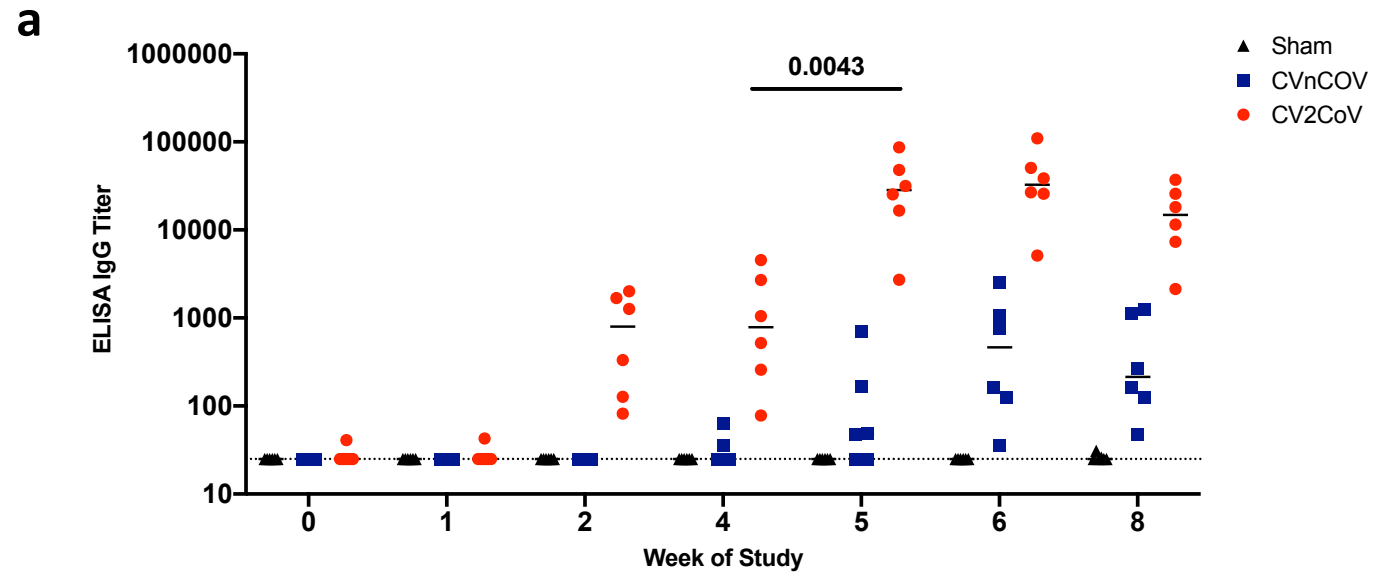


Figure 2

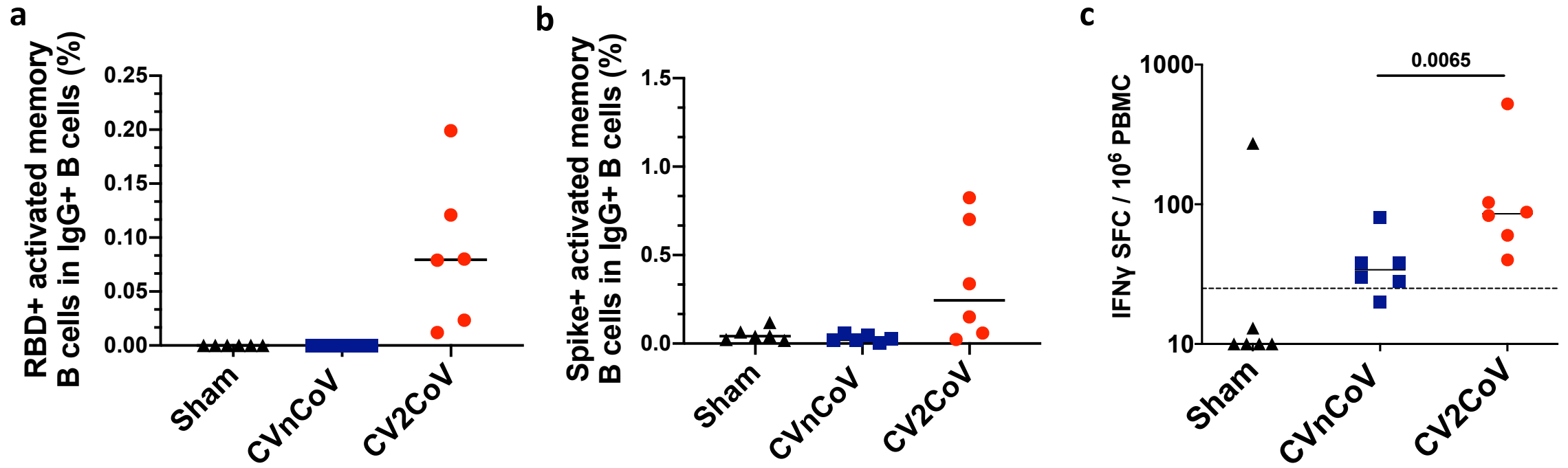
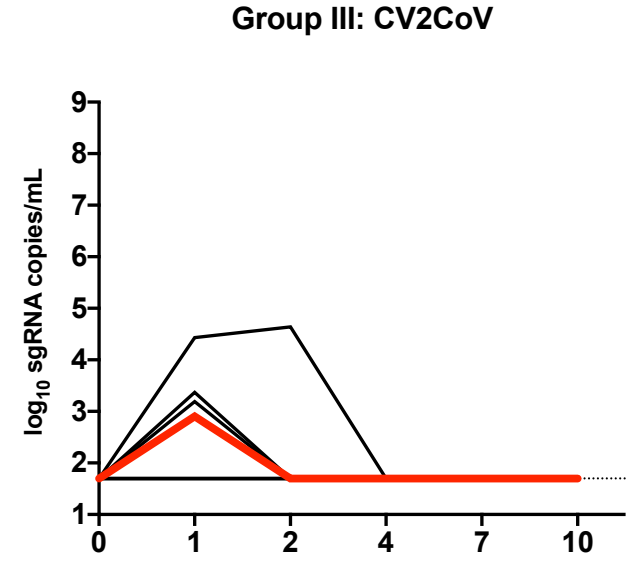
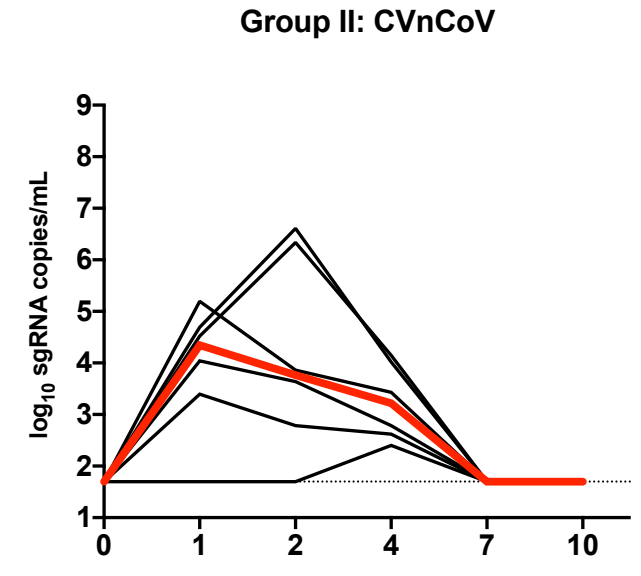
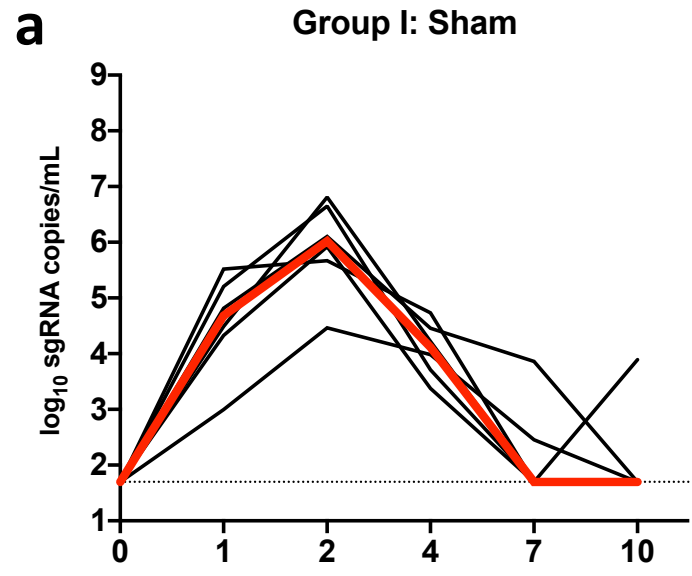


Figure 3

BAL



Nasal Swab

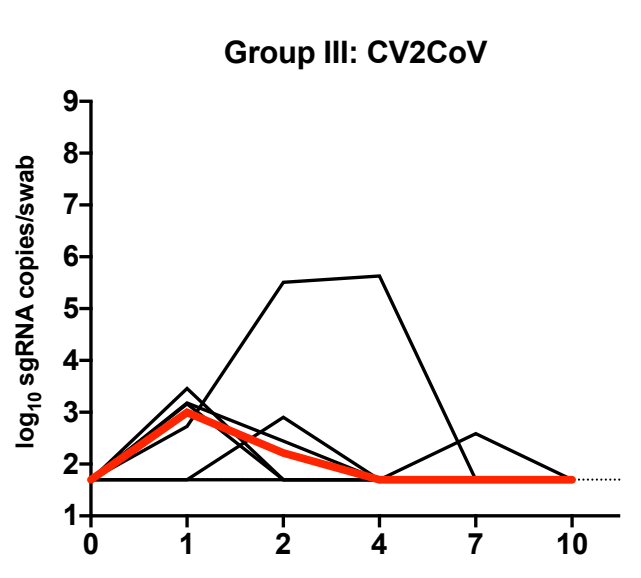
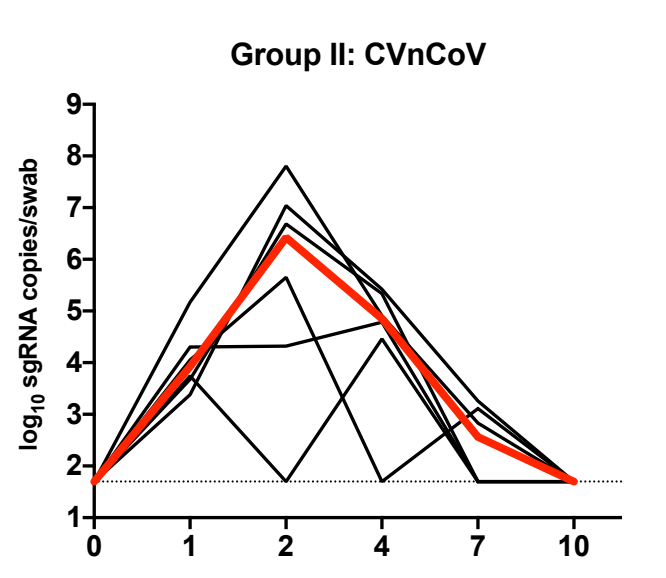
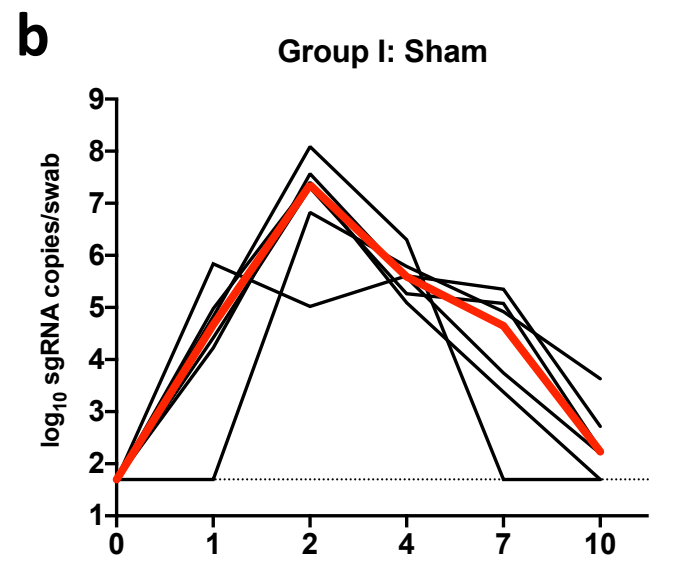


Figure 4

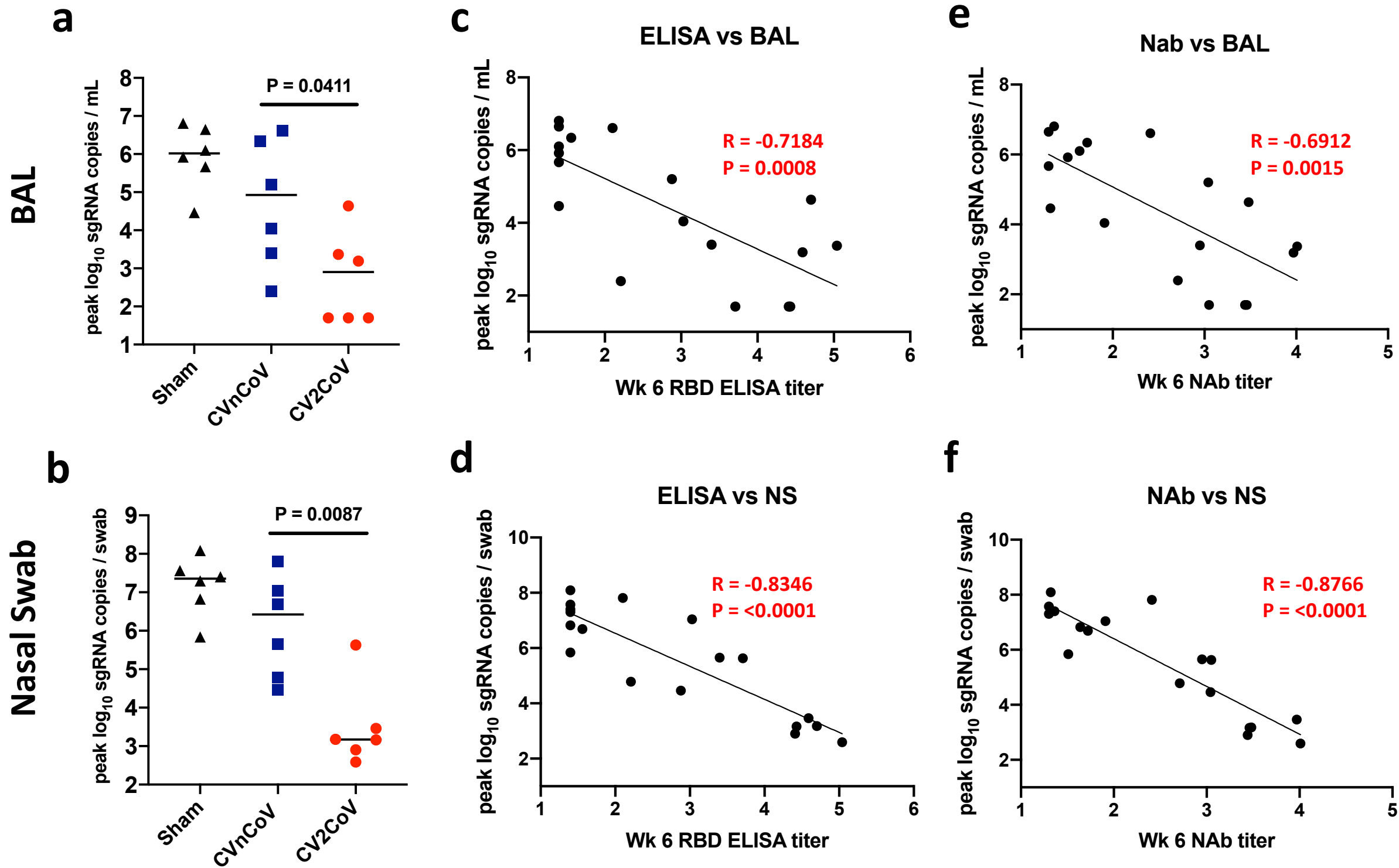
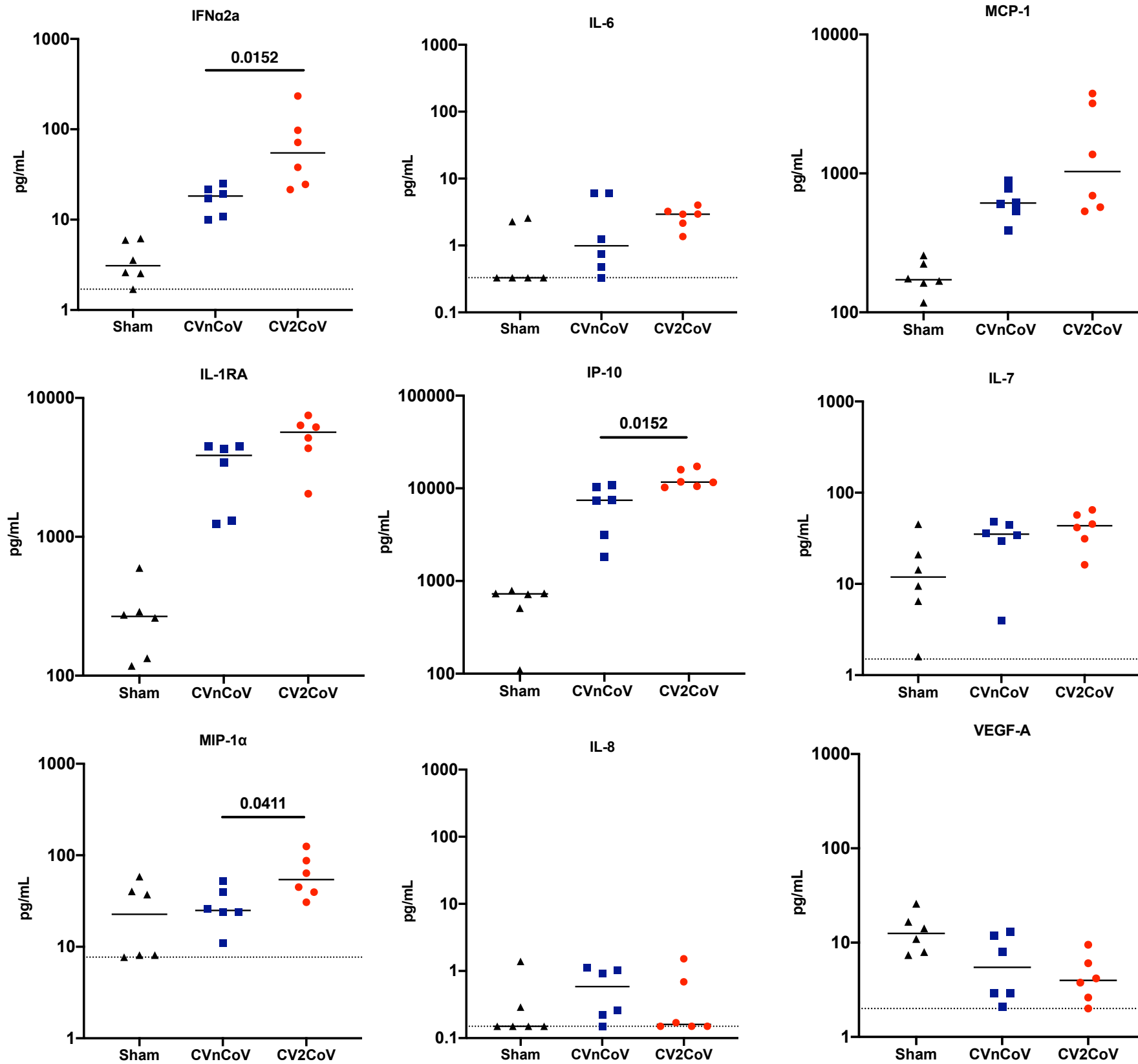
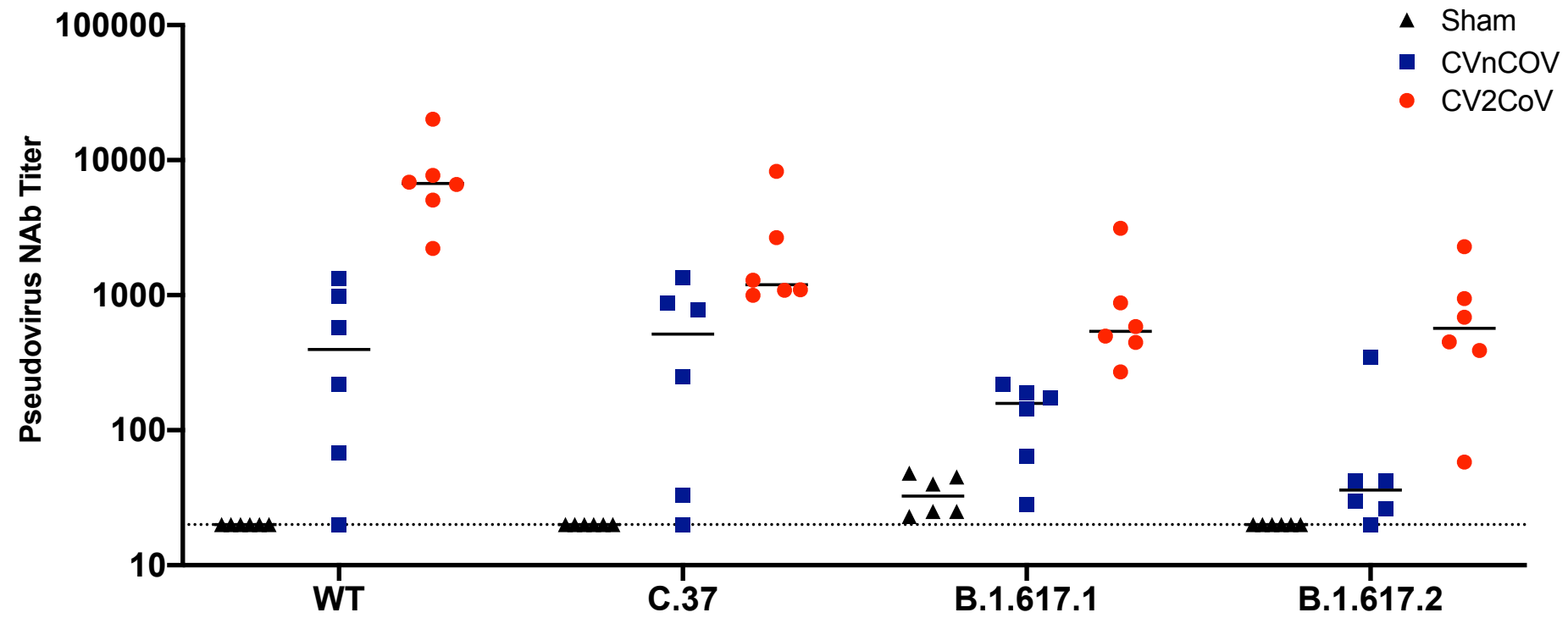


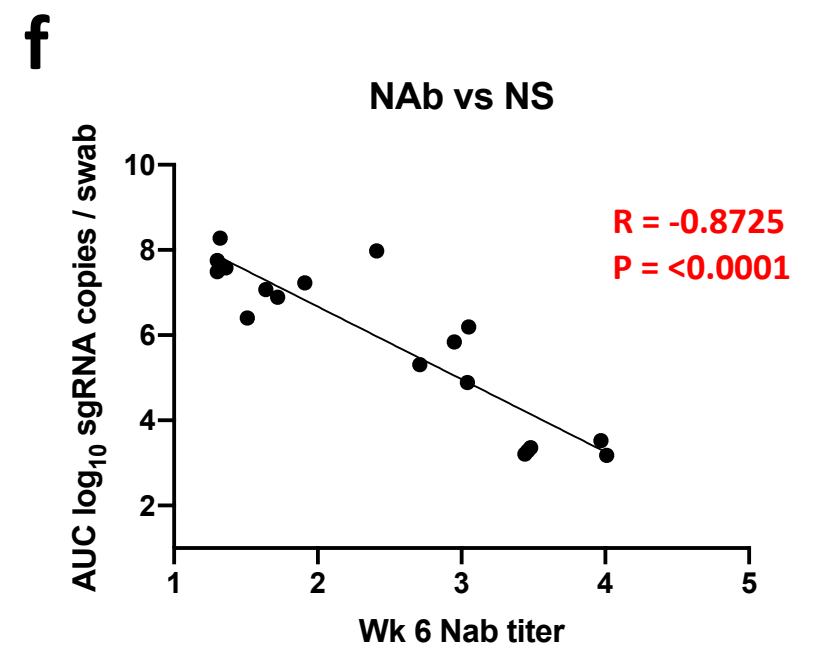
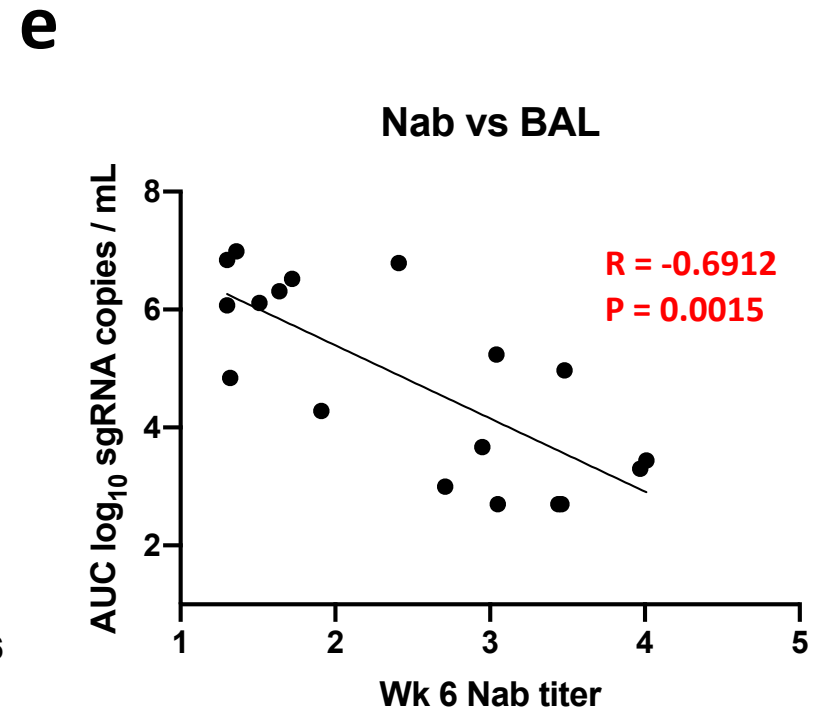
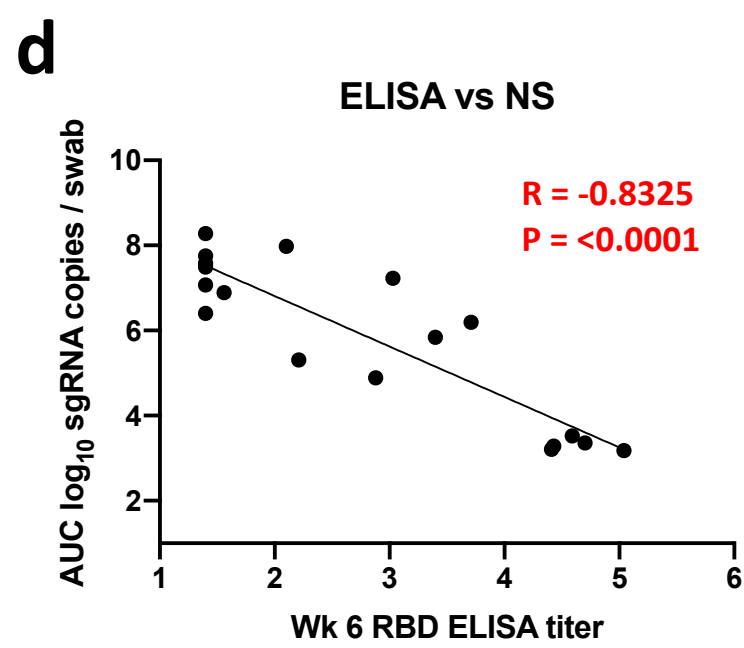
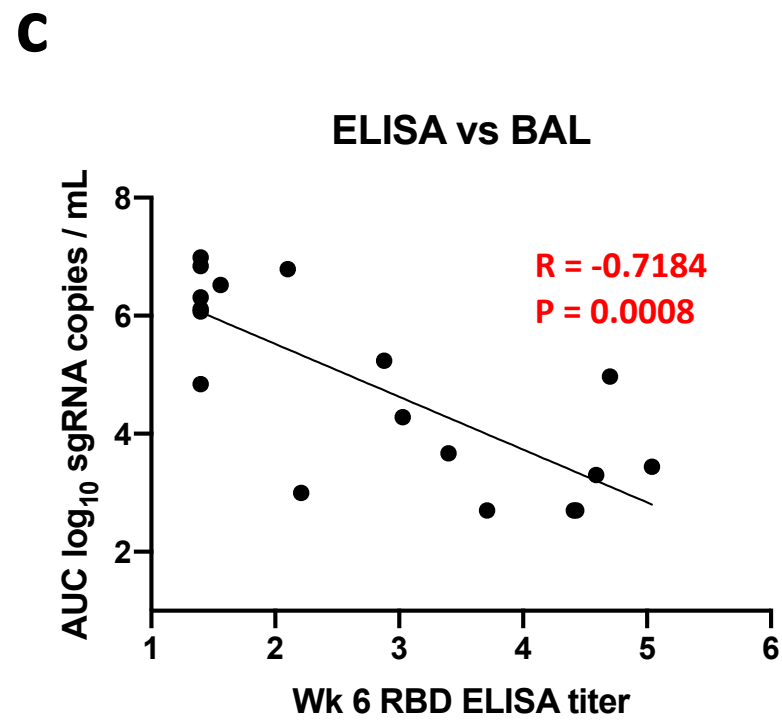
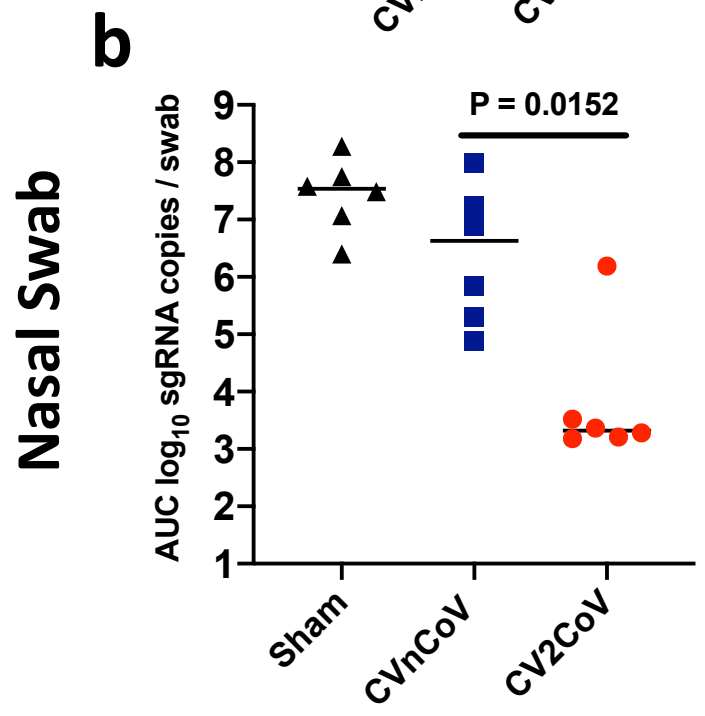
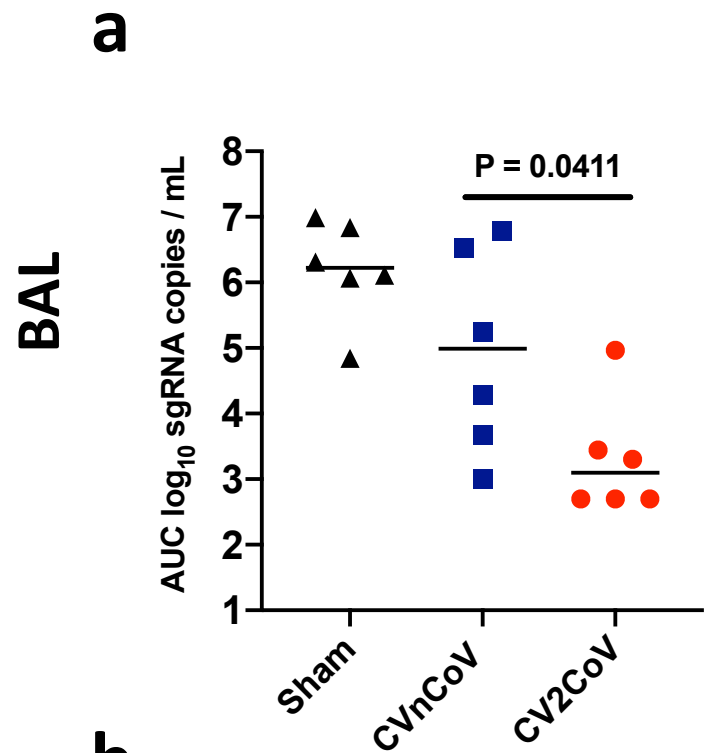
Figure 5



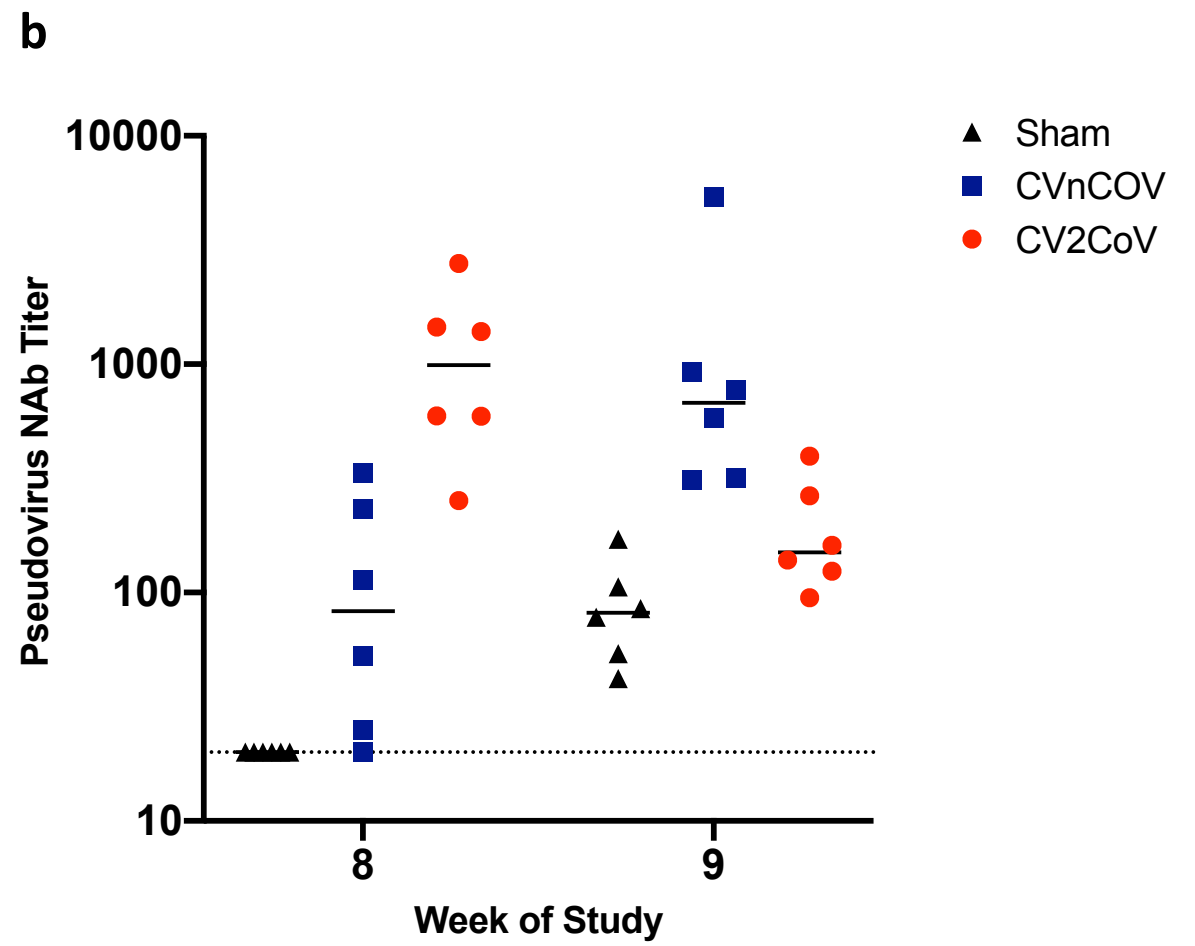
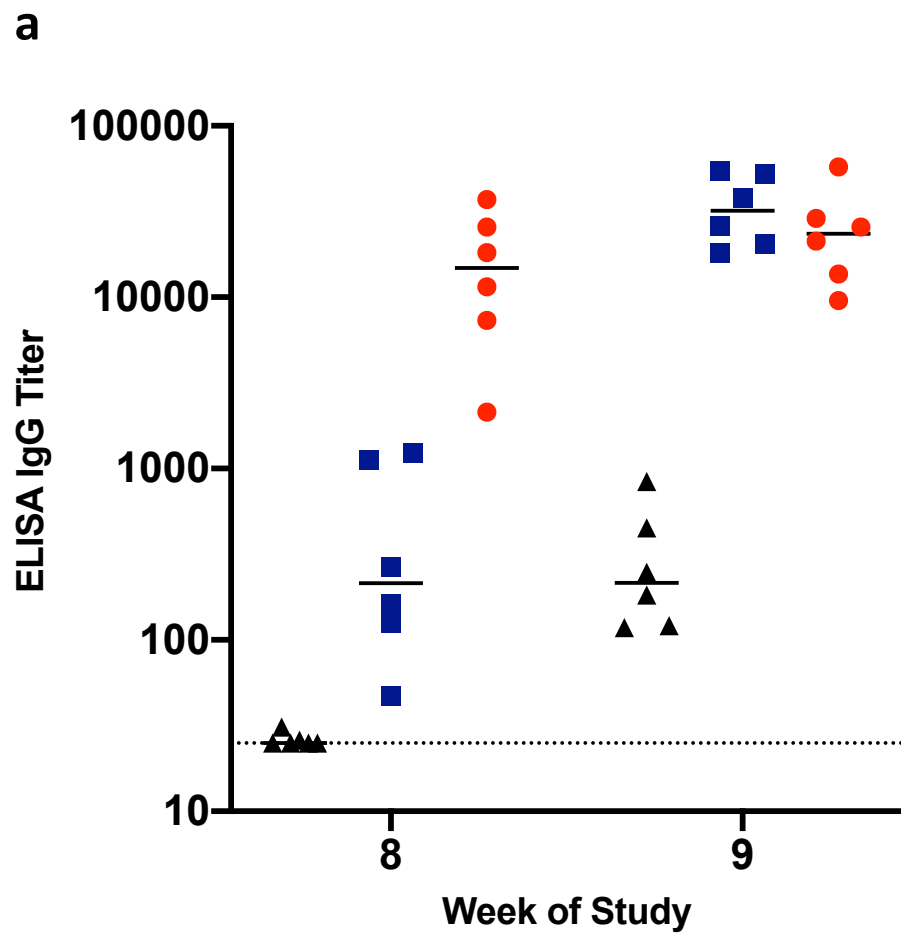
Extended Data Figure 1

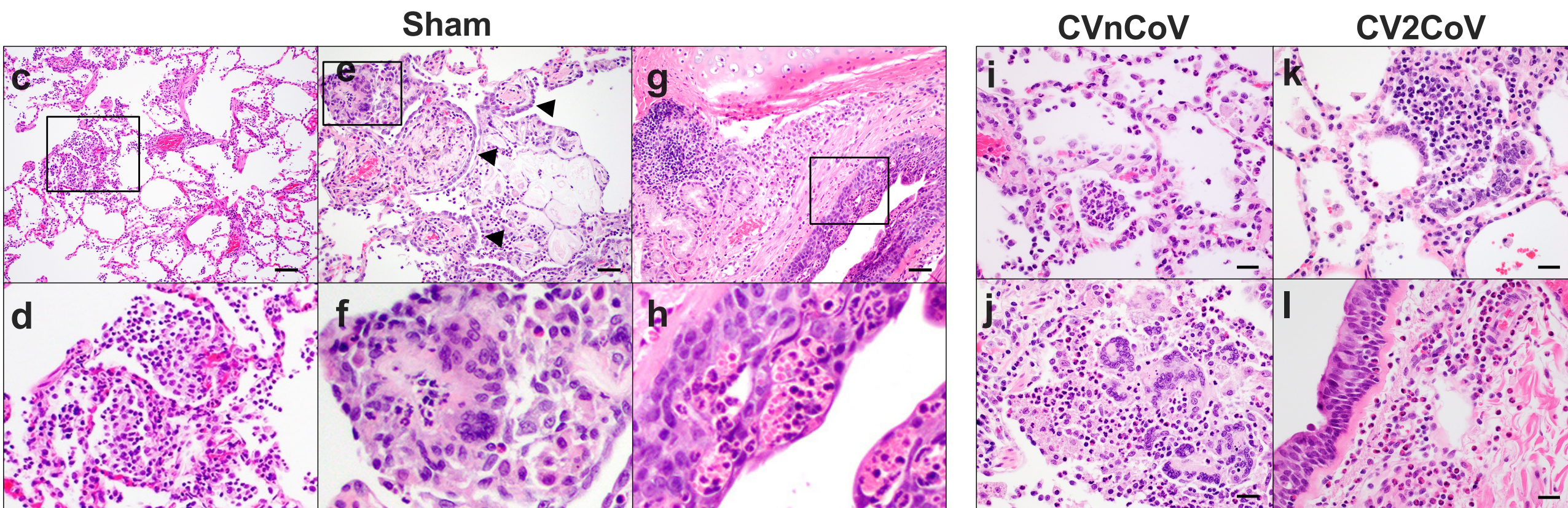
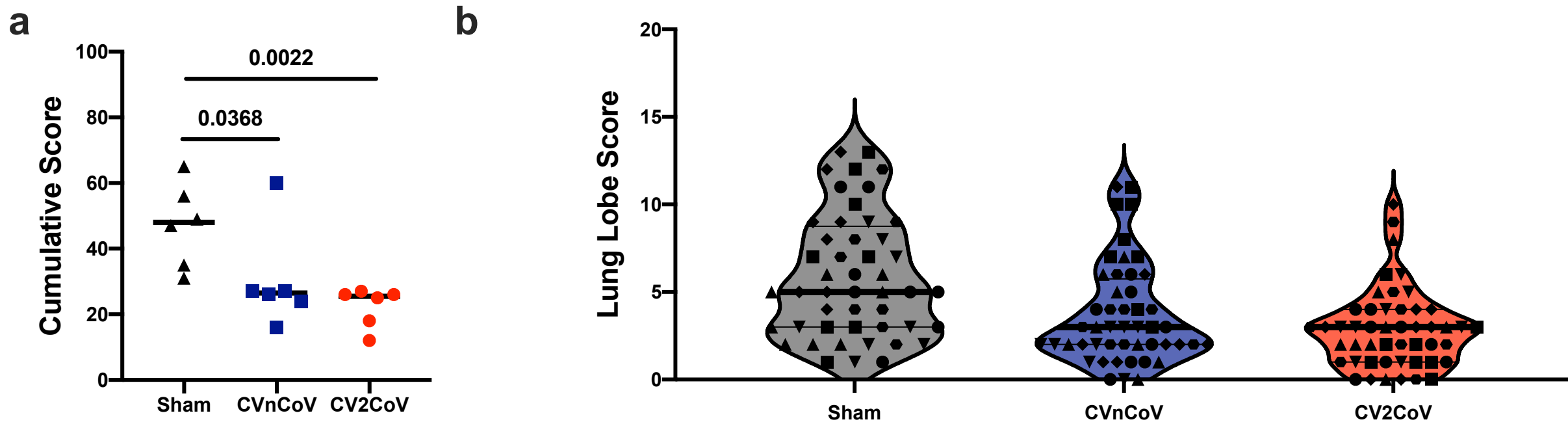


Extended Data Figure 2



Extended Data Figure 3





Extended Data Figure 5